Original Article

MOLECULAR METABOLISM

Adipocyte Gs but not Gi signaling regulates whole-body glucose homeostasis

Alexandre Caron [1,*], Ryan P. Reynolds [1], Carlos M. Castorena [1], Natalie J. Michael [1], Charlotte E. Lee [1], Syann Lee [1], Rebecca Berdeaux [2], Philipp E. Scherer [3], Joel K. Elmquist [1,]**

ABSTRACT

Objective: The sympathetic nervous system (SNS) is a key regulator of the metabolic and endocrine functions of adipose tissue. Increased SNS outflow promotes fat mobilization, stimulates non-shivering thermogenesis, promotes browning, and inhibits leptin production. Most of these effects are attributed to norepinephrine activation of the Gs-coupled beta adrenergic receptors located on the surface of the adipocytes. Evidence suggests that other adrenergic receptor subtypes, including the Gi-coupled alpha 2 adrenergic receptors might also mediate the SNS effects on adipose tissue. However, the impact of acute stimulation of adipocyte Gs and Gi has never been reported.

Methods: We harness the power of chemogenetics to develop unique mouse models allowing the specific and spatiotemporal stimulation of adipose tissue Gi and Gs signaling. We evaluated the impact of chemogenetic stimulation of these pathways on glucose homeostasis, lipolysis, leptin production, and gene expression.

Results: Stimulation of Gs signaling in adipocytes induced rapid and sustained hypoglycemia. These hypoglycemic effects were secondary to increased insulin release, likely consequent to increased lipolysis. Notably, we also observed differences in gene regulation and *ex vivo* lipolysis in different adipose depots. In contrast, acute stimulation of Gi signaling in adipose tissue did not affect glucose metabolism or lipolysis, but regulated leptin production.

Conclusion: Our data highlight the significance of adipose Gs signaling in regulating systemic glucose homeostasis. We also found previously unappreciated heterogeneity across adipose depots following acute stimulation. Together, these results highlight the complex interactions of GPCR signaling in adipose tissue and demonstrate the usefulness of chemogenetic technology to better understand adipocyte function.

Keywords Adipose tissue; DREADD; Glucose; Insulin; Leptin; Lipolysis

1. INTRODUCTION

G protein-coupled receptors (GPCRs) are among the most intensively studied pharmacological targets [1—3]. As their names imply, GPCRs interact with G proteins located in the plasma membrane. When a ligand binds to the GPCR, it causes a conformational change that triggers the interaction between the GPCR and a nearby G protein. There are four main families of G proteins: Gi/Go, Gq, Gs, and G12 [2,3]. The cAMP and the phosphatidylinositol pathways are the two principal signal transduction pathways that rely on GPCR activation [2,3].

Because of their pleiotropic effects on energy and glucose homeostasis, GPCRs expressed in white adipose tissue (WAT) and brown adipose tissue (BAT) are considered potential targets for the treatment of metabolic diseases [4—6]. WAT and BAT are organs specialized for lipid storage and non-shivering thermogenesis, respectively [7,8]. Under specific physiological conditions, clusters of brown-like ('brite') adipocytes can develop within WAT depots, a process referred to as the browning of WAT. The development of beige adipose tissue (BeAT) was suggested to play an important role in energy and glucose homeostasis [8,9]. The sympathetic nervous system (SNS) is a key regulator of the metabolic and endocrine functions of adipose tissue [10]. In particular, increased SNS outflow promotes fat mobilization [11], stimulates non-shivering thermogenesis [12], promotes browning [9], and inhibits leptin production [10]. Moreover, SNS action is differentially regulated in each adipose depot. For example, cold exposure increases both WAT lipolysis and BAT thermogenesis [13,14], whereas fasting increases WAT lipid mobilization but reduces BAT activity [15]. However, we still do not fully understand the regional differences in SNS stimulation of adipose tissue metabolism.

[1]Department of Internal Medicine, Division of Hypothalamic Research, University of Texas Southwestern Medical Center, Dallas, TX, USA [2]Department of Integrative Biology and Pharmacology, Center for Metabolic and Degenerative Diseases at the Brown Foundation, Institute of Molecular Medicine, McGovern Medical School at The University of Texas Health Science Center at Houston (UTHealth), Graduate Program in Biochemistry and Cell Biology, MD Anderson Cancer Center-UTHealth Graduate School of Biomedical Sciences, Houston, TX, USA [3]Touchstone Diabetes Center, Department of Internal Medicine, University of Texas Southwestern Medical Center, Dallas, TX, USA

*Corresponding author. Department of Internal Medicine, Division of Hypothalamic Research, University of Texas Southwestern Medical Center, 5323 Harry Hines Blvd, Dallas, TX, 75390-9077, USA. E-mail: Alexandre.Caron@UTSouthwestern.edu (A. Caron).

**Corresponding author. Department of Internal Medicine, Division of Hypothalamic Research, University of Texas Southwestern Medical Center, 5323 Harry Hines Blvd, Dallas, TX, 75390-9077, USA. E-mail: Joel.Elmquist@UTSouthwestern.edu (J.K. Elmquist).

Received May 14, 2019 • Revision received June 20, 2019 • Accepted June 20, 2019 • Available online 22 June 2019

https://doi.org/10.1016/j.molmet.2019.06.019

In rodents, most of the effects of the SNS on adipose tissue are attributed to norepinephrine (NE) activation of Gs-coupled beta 3 adrenergic receptors (ADRB3) located at the surface of the adipocytes [16,17]. Evidence also indicates that Gs-coupled beta 1 adrenergic receptors (ADRB1) are important for SNS stimulation of thermogenesis [18]. A prevalent model predicts that activation of adipose β-adrenergic receptors promotes a molecular cascade that triggers the accumulation of cAMP, which results in protein kinase A (PKA) activation [16,17]. In turn, PKA activates the canonical lipolytic pathway, which leads to activation of thermogenesis in BAT through allosteric activation of uncoupling protein 1 (UCP1) by fatty acids [17,19]. In rodents, pharmacological stimulation of ADRB3 mimics these effects and results in the reduction of blood glucose [14,20,21]. Supporting the importance of Gs signaling in mediating these effects, deletion of the stimulatory alpha subunit *Gnas* in adipocytes affects glucose metabolism and thermogenesis [22,23]. In addition to ADRB3, adipocytes express a number of other Gs-coupled receptors whose activation promotes similar pathways and effects [19,24]. Evidence also suggests that the Gi/o-coupled alpha 2 adrenergic receptors (ADRA2) may play a role in regulating metabolism. For example, they oppose the stimulation of lipolysis by ADRB3 by reducing cAMP levels [25,26]. Moreover, the ADRB3/ADRA2 balance has been proposed to be key for regulating leptin production [27,28] and human adipocytes express higher amount of ADRA2A compared to ADRB3 [25]. However, much of our knowledge on the roles of adipose GPCRs is based on systemic treatment with pharmacological agents or whole-body knock-out mouse models. As such, novel genetic tools allowing specific manipulation of GPCR signaling in adipose tissue are needed.

Designer Receptors Exclusively Activated by Designer Drugs (DREADDs) are chemogenetically-engineered proteins that allow spatial and temporal control of G protein signaling *in vivo* [29]. Originally developed to control neuronal activity [29], DREADDs are emerging as key tools to control peripheral organs, including liver [30,31], heart [32], and pancreas [33]. However, these tools have never been used to manipulate GPCR signaling in adipose tissue. Here, we used chemogenetic tools allowing acute stimulation of Gs or Gi signaling specifically in adipocytes. We report that Gs, but not Gi, signaling is a potent regulator of systemic glucose homeostasis.

2. MATERIAL AND METHODS

2.1. Animals

Animal work described in this manuscript has been approved and conducted under the oversight of the UT Southwestern Institutional Animal Care and Use Committee (IACUC). Mice were housed at an ambient temperature of 23 ± 1 °C and maintained on a 12 h light/dark cycle (lights on 0600–1800) and fed with normal mouse chow diet (Envigo, 2016 Teklad Global 16% protein and 4% fat rodent diet). All experiments were conducted using 8-14-week-old males.

2.2. Generation of *Adipoq*-GsD mice

To generate mice in which Gs signaling in adipose tissue is acutely stimulated following CNO administration (*Adipoq*-GsD), a C57BL/6J congenic version of the adiponectin (*Adipoq*)-Cre mouse (The Jackson Laboratory, Stock No: 028020) [34] was crossed with Cre-dependent Gs-coupled DREADD (GsD) C57BL/6J mice (MGI accession number 5696731) [30]. The following genotyping primers were used: 5′-CTC GAA GTA CTC GGC GTA GG-3′ and 5′-CTT GGC AAT CCG GTA CTG TT-3′ for the GsD allele (206-bp product), and 5′-AAG GGA GCT GCA GTG GAG TA and 5′-CCG AAA ATC TGT GGG AAG TC for the wild-type (WT) allele (297-bp product).

2.3. Generation of *Adipoq*-GiD mice

To generate mice in which Gi signaling in adipose tissue is acutely stimulated following CNO administration (*Adipoq*-GiD), a C57BL/6J congenic version of the adiponectin (*Adipoq*)-Cre mouse (The Jackson Laboratory, Stock No: 028020) [34] was crossed with Cre-dependent Gi-coupled DREADD (hM4Di) C57BL/6NJ mice (The Jackson Laboratory, Stock No: 026219) [35]. The following genotyping primers were used: 5′-TCA TAG CGA TTG TGG GAT GA-3′ and 5′-CGA AGT TAT TAG GTC CCT CGA C-3′ for the hM4Di allele (200-bp product), and 5′-AAG GGA GCT GCA GTG GAG TA and 5′-CCG AAA ATC TGT GGG AAG TC for the wild-type (WT) allele (297-bp product).

2.4. Effects of chemogenetic stimulation of adipose tissue on glucose homeostasis

Adipoq-GsD, *Adipoq*-GiD mice and their respective littermate controls were fasted for 4 h (0600–1000) before receiving an intraperitoneal injection (IP) of clozapine N-oxide (CNO, 1 mg/kg, Sigma C0832). Tail vein blood glucose levels were then monitored for up to 3 h using a glucometer (Bayer's Contour Blood Glucose Monitoring System; Leverkusen, Germany). To determine the impact of chemogenetic Gs stimulation on glucose clearance, *Adipoq*-GsD mice and their littermate controls were fasted for 4 h (0600–1000) before we co-administrated (IP) CNO (1 mg/kg) and glucose (1.5 mg/kg, Sigma 49163-100 ML). To compare the hypoglycemic effects of chemogenetic Gs stimulation to insulin, *Adipoq*-GsD mice and their littermate controls were fasted for 4 h (0600–1000) before we co-administrated (IP) CNO (1 mg/kg) and human recombinant insulin (0.75 mU/kg, Eli Lilly).

2.5. Effects of chemogenetic stimulation of adipose tissue on plasma insulin, leptin, NEFA and glycerol

Mice and their littermate controls were fasted for 4 h (0600–1000) before receiving CNO (1 mg/kg). For insulin levels, blood from tail vein was collected before, and 30 min after, the injection into EDTA tubes. For leptin levels, blood from the tail vein was collected before, and up to 2 h after, the injection in EDTA tubes. Plasma was isolated by centrifugation (4000 g × 10 min at 4 °C) and was stored at −80 °C for further biochemical analyses. Plasma insulin (Mouse Ultrasensitive Insulin ELISA, ALPCO, 80-INSMSU-E01) and leptin (Mouse/Rat Leptin ELISA, ALPCO, 22-LEPMS-E01) levels were measured following manufacturer recommendations. For NEFA and glycerol levels, blood from tail vein was collected before, and up to 2 h after, the injection. Plasma was isolated by centrifugation and NEFA and glycerol quantified immediately using colorimetry assays (FUJIFILM Wako Diagnostics-NEFA Reagent, 999-34691, 995-34791, 991-34891, 993-35191; Sigma Free Glycerol Reagent, F6428).

2.6. Western blotting

Adipoq-GsD mice and littermate controls were fasted for 4 h and then injected with CNO (1 mg/kg). Epididymal white adipose tissue (eWAT) from *Adipoq*-GsD mice and littermate controls were collected and frozen 30 min later. Using 1.4 mm ceramic spheres (Lysing Matrix D; MP biomedical), tissues were homogenized (30 s × 6000 rpm) in ice-cold lysis buffer composed of T-PER buffer (Thermo Scientific, 78510), 1% (v/v) of protease inhibitor cocktail (P8340-5 ML, Sigma), and phosphatase inhibitor tablets PhosSTOP (Sigma 4906837001). Tissues were placed on a rotor at 4 °C for 1 h and then the soluble fractions of the tissue lysates were isolated by centrifugation (10,000 × *g*, 4 °C for 10 min). The supernatant was carefully pipetted into a new tube and the protein concentration was measured via BCA protein assay (Life Technologies). Equal amounts of total protein (40 μg) per sample were

diluted with appropriate volume of Laemmle sample buffer (2X concentrated; 4% SDS, 10% 2-mercaptoethanol, 20% glycerol, 0.004% bromophenol blue and 0.125 M pH6.8 Tris—HCl) heated for 5 min at 95 °C, separated via SDS-PAGE 4—15% Tris—HCl gels (Bio-Rad, Hercules, CA), transferred to nitrocellulose membranes (Trans-blot turbo, Bio-Rad, Hercules, CA), and incubated with the appropriate primary antibody overnight at 4 °C. The following primary antibodies were used: Akt (Cell Signaling Technology, 4691, dilution 1:1000), phospho-AKT S473 (Cell Signaling Technology, 9271, dilution 1:1000). Membranes were then incubated with florescent secondary antibodies (IRDye 800CW Goat anti-Rabbit IgG; Li-Cor Bioscience) and protein band fluorescence was quantified using the Li-Cor Odyssey Image studio Version 4.0 (Li-Core Bioscience).

2.7. Quantitative real-time PCR

Adipoq-GsD mice and littermate controls were injected with CNO (1 mg/kg) after a 4 h fast, and tissues were collected 6 h later. Total mRNA was isolated from eWAT, inguinal white adipose tissue (iWAT), and interscapular brown adipose tissue (BAT) using the Aurum™ Total RNA Fatty and Fibrous Tissue Kit (Bio-Rad, 732—6830). RNA concentration was estimated from absorbance at 260 nm cDNA synthesis was performed using the iScript Advanced cDNA Synthesis Kit (Bio-Rad, 172—5038). mRNA extraction and cDNA synthesis were performed following the manufacturer's instructions. cDNA was diluted in DNase-free water before quantification by real-time PCR. Relative quantification of gene expression was performed on diluted cDNA in duplicate samples using a CFX384 touchTM real-time PCR (Bio-Rad). Fold differences in targeted mRNA expression were calculated using the 2-delta cycle threshold method and data were normalized to beta-microglobulin (*B2m*) expression. TaqMan® gene expression assays for *B2m* (Mm00437762_m1), *Sik1* (Mm00440317_m1), *Lipe* (Mm00 495359_m1), *Dgat1* (Mm00515643_m1), *Ppargc1a* (Mm01208 835_m1), *Ucp1* (Mm01244861_m1), *Tbk1* (Mm00451150_m1), *Lep* (Mm00434759_m1), *Adipoq* (Mm00456425_m1), *Adrb3* (Mm02601 819_g1), *Gnas* (Mm01242435_m1), *Gnal* (Mm01258217_m1), *Gnai1* (Mm01165301_m1), *Gnai2* (Mm00492379_g1), *Gnai3* (Mm00802 670_m1), and *Gnaz* (Mm01150269_m1) were purchased from ThermoFisher Scientific. Integrated DNA Technologies (IDT)'s PrimerQuest Software was used to design primers and probes containing a ZEN™ quencher, a 3′ Iowa Black® FQ quencher and a 5′ 6-fluorescein (FAM) to evaluate *GsD* and *GiD* expression. For *GsD*: primer 1 (5 nM) 5′-ATG CCA GGA AGC CAG TAA AG-3′, primer 2 (5 nM): 5′-GTT GGG CAG CTA CAA CATT TC-3′, probe (2.5 nM) 5′/56-FAM/TTC TCC TCA/ZEN/AAC GAC ACC TCC AGC/3IABkFQ/-3′. For *GiD*: primer 1 (5 nM) 5′-CGC TAT GAG ACG GTG GAA AT-3′, primer 2 (5 nM) 5′-CGC TAT GAG ACG GTG GAA AT-3′, probe (2.5 nM) 5′/56-FAM/ATC ACC AGG/ZEN/ATG TTG CCC ACGA/3IABkFQ/-3′.

2.8. Evaluation of lipolysis and leptin release in adipose organ explants

We used a modified version of a well-established lipolysis assay [36] to evaluate NEFA, glycerol, and leptin release from adipose organ explants. Briefly, eWAT, iWAT, and BAT from *Adipoq*-GsD, *Adipoq*-GiD and respective littermate controls were surgically removed and cut in ~20 mg pieces. The pieces were put in a 96-well plate containing 200 μl of prewarmed (37 °C) DMEM no phenol red (Gibco A1443001). The pieces were then incubated at 37 °C (5% CO2, and 95% humidified atmosphere) for one hour (baseline) in DMEM containing 2% fatty acid (FA)-free bovine serum albumin (BSA, Sigma, A8806) and 0.1% glucose (Sigma 49163). To avoid re-esterification of FA and glycerol, each well also contained 5 μM of the acyl-CoA synthetases inhibitor triacsin C (Tocris 2472). At the end of the hour, the pieces were transferred to a new 96-well plate containing fresh medium with 1 μM CNO (C0832, Sigma) and incubated for another hour (stimulated). The incubation media from baseline and stimulated conditions were then used to evaluate NEFA release by colorimetry (FUJIFILM Wako Diagnostics-NEFA Reagent, 999-34691, 995-34791, 991-34891, 993-35191), glycerol release by colorimetry (F6428, Sigma), and leptin release by ELISA (Mouse/Rat Leptin ELISA, ALPCO, 22-LEPMS-E01). NEFA, glycerol, and leptin release were then calculated based as a percentage compared to baseline.

2.9. Assessment of body composition

Fat mass and lean mass were assessed by nuclear magnetic resonance (NMR) spectroscopy using a Bruker Minispec mq10 NMR 0.23T/10 MHz.

2.10. Metabolic cages

A combined indirect calorimetry system (LabMaster System, TSE Systems Inc.) was used to evaluate the impacts of stimulating GsD and GiD selectively in adipose tissues on different metabolic parameters. Experimental animals were acclimated for 5 days in a metabolic chamber with food and water. Food intake, oxygen consumption (VO2), respiratory exchange ratio (RER), and locomotor activity were measured for 24 h after animals were injected with CNO (1 mg/kg) in the morning at 1000. Locomotion was measured using a multi-dimensional infrared light beam system.

2.11. Histology

Samples from eWAT, iWAT, and BAT were taken 24 h following CNO (1 mg/kg) and were immediately fixed overnight in 10% formalin. Samples were then dehydrated, embedded in paraffin, and cut into 5 μm-thick sections. Sections were stained with hematoxylin and eosin (H&E) to perform general histology. All pictures were taken at a magnification of 20× on a Zeiss Axioskop 2 microscope connected to a digital camera (AxioCam; Zeiss, Thornwood, NY). Only the sharpness, contrast, and brightness were adjusted.

2.12. Treatment with CL 316,243

C57BL6/J mice (obtained from the UTSW breeding core) fasted for 4 h (0600—1000) and then given an injection of the ADRB3 agonist CL 316,243 (Sigma, C5976, high dose - 1 mg/kg or low dose - 0.1 mg/kg, IP). Blood glucose was measured for the next 2 h. To test whether GiD stimulation blocks the effects of CL 316,243 on glucose levels, *Adipoq*-GiD mice and littermate controls were fasted for 4 h (0600—1000) before receiving an injection of CNO (1 mg/kg, IP). Thirty minutes later, a low dose of CL 316,243 (0.1 mg/kg, IP) was given and blood glucose was measured for the next 2 h.

2.13. Statistical analysis

Data are expressed as the mean ± SEM. Comparisons between two experimental conditions were analyzed by Student's unpaired t test. Two-way ANOVA followed by Tukey post-hoc test was used to compare more than two experimental conditions. All statistical tests were performed using GraphPad Prism (version 7.0), and $p < 0.05$ was considered statistically significant.

3. RESULTS

3.1. Chemogenetic stimulation of Gs signaling in adipocytes induces hypoglycemia

It was recently reported that chemogenetic stimulation of Gs signaling in hepatocytes increases blood glucose by activating cAMP [30]. This approach demonstrated that Gs-DREADD (GsD) can be readily used to mimic GsPCR activation, such as the glucagon receptor, in the liver [30,37]. Because of the importance of the Gs-coupled beta adrenergic receptors and downstream cAMP signaling in adipocytes [4,10,38], we aimed to determine whether this approach could be used to study the impact of Gs signaling activation in adipose tissue. A C57BL/6J congenic version of the adiponectin (*Adipoq*)-Cre mouse [34] was crossed with Cre-dependent Gs-coupled DREADD (GsD) mice [30] to generate mice in which Gs signaling is acutely stimulated following CNO administration (*Adipoq*-GsD). Validation of the expression of the *GsD* in eWAT, iWAT and BAT is shown in Fig. S1A. Expression of *Adrb3* was not significantly altered in these different adipose depots (Fig. S1B). Likewise, expression of endogenous Gs proteins (GNAS Complex Locus, *Gnas* and G Protein Subunit Alpha L, *Gnal*) were not significantly altered (Fig. S1C—D). Based on evidence that *Gnas* deficiency in adipose tissue improves glucose metabolism [22], we evaluated the impact of chemogenetic stimulation of Gs signaling in adipocytes on glucose homeostasis. As shown in Figure 1A—D, CNO induced a rapid and persistent reduction in blood glucose in *Adipoq*-GsD mice compared to their littermate controls. Strikingly, blood glucose was 41% lower than baseline, with an average of 59.25 $\pm$ 5.03 versus 165.70 $\pm$ 30.41 mg/dL, for 3 h following CNO administration (Figure 1C). When CNO was co-administrated with glucose, we found that the glucose clearance was also drastically improved (Figure 1E—F). When CNO was co-administrated with recombinant insulin, we did not find any additional hypoglycemic effects of CNO over insulin (Figure 1G—H). Importantly, these effects were independent of changes in body composition, food intake or energy expenditure (Fig. S2A—E). Together, these results indicate that stimulation of Gs signaling in adipocytes potently increases glucose clearance and induces hypoglycemia, independent of alterations in energy balance.

3.2. Chemogenetic stimulation of Gs signaling in adipocytes increases insulin levels through an adipose tissue-pancreas crosstalk

Because the magnitude by which CNO reduced blood glucose in *Adipoq*-GsD mice was similar to the hypoglycemic effects of insulin in littermate controls (Figure 2A), we next assessed insulin levels following the chemogenetic stimulation. As shown in Figure 2B, plasma insulin went up more than 4-fold 30 min following CNO treatment in *Adipoq*-GsD mice but not littermate controls. This was concomitant with an increase in insulin signaling, as assessed by p-Akt in eWAT (Figure 2C). These observations are in line with previous studies reporting increased insulin levels after acute treatment with CL316,243 [5,39], an agonist of Gs-coupled ADRB3. Based on evidence that CL316,243 increases lipolysis and that its incretin effects are dependent on non-esterified fatty acids (NEFA) release [5,39], we next evaluated the impact of stimulating adipocyte Gs signaling on NEFA levels. We found that CNO dramatically increased plasma NEFA levels within 15 min (Figure 2D). Importantly, blood glucose levels negatively mirrored the NEFA levels in *Adipoq*-GsD animals, as supported by a significant negative correlation between glucose and NEFA levels 30 min after CNO administration (Figure 2E—G). These data suggest that the hypoglycemic effects of acute stimulation of Gs

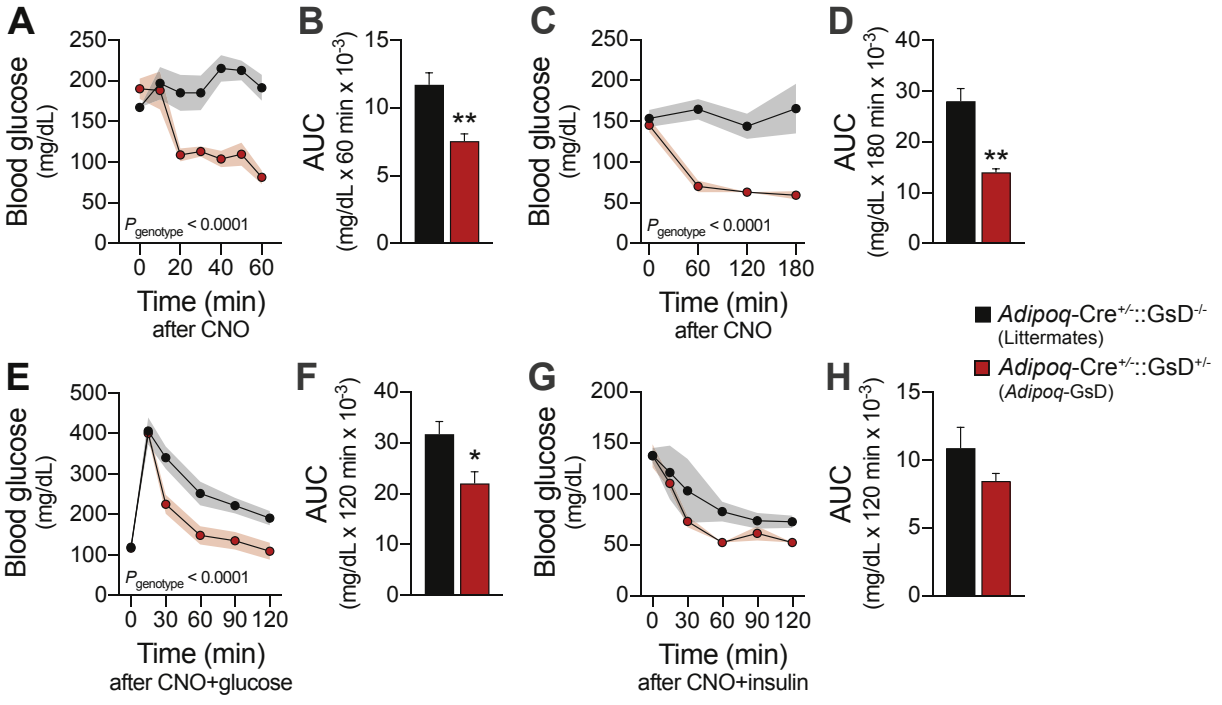

Figure 1: Chemogenetic stimulation of Gs signaling in adipocytes induces hypoglycemia. (A) Blood glucose measured every 10 min for an hour following CNO (1 mg/kg) in *Adipoq*-GsD and littermate controls. (B) Area under the curve (AUC) for A. (C) Blood glucose measured every hour for 3 h following CNO (1 mg/kg) in *Adipoq*-GsD and littermate controls. (D) AUC for C. (E) Blood glucose following co-administration of CNO (1 mg/kg) and D-glucose (1.5 mg/kg). (F) AUC for E. (G) Blood glucose following co-administration of CNO (1 mg/kg) and recombinant human insulin (0.75 mU/kg). (H) AUC for G. The data are expressed as the mean $\pm$ SEM for n = 4—11. * indicates $p < 0.05$ and ** indicates $p < 0.01$ versus littermate controls. The annotated p value was calculated by two-way ANOVA.

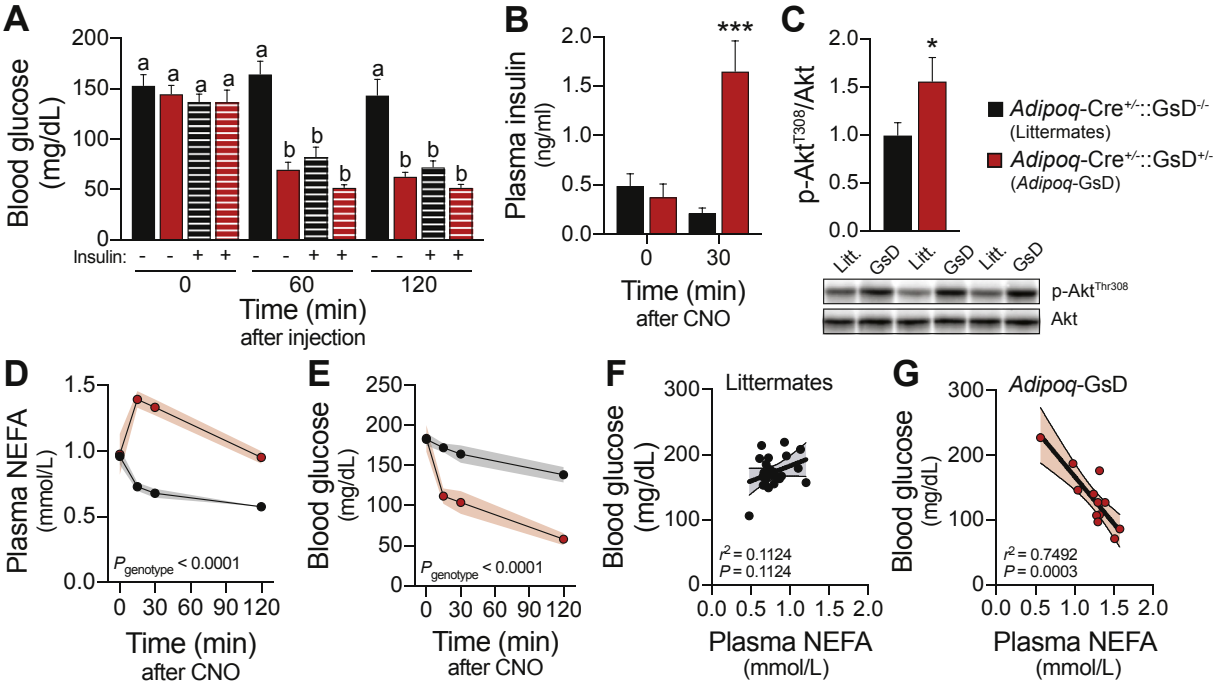

Figure 2: Chemogenetic stimulation of Gs signaling in adipocytes increases insulin levels through an adipose tissue-pancreas crosstalk. (A) Comparison of blood glucose following co-administration of CNO (1 mg/kg) +/− insulin (0.75 mU/kg). Stripped columns represent groups receiving both CNO and insulin. (B) Plasma insulin before and 30 min after CNO (1 mg/kg) administration. (C) Representative western blot showing the expression of p-Akt (Thr308) in eWAT of *Adipoq*-GsD and littermate controls. Akt was used as a loading control and representative image is shown. (D) Plasma NEFA levels following CNO (1 mg/kg). (E) Blood glucose levels during D. (F) Correlation between blood glucose and NEFA levels in littermates and (G) *Adipoq*-GsD over the first 30 min of D-E. The data are expressed as the mean ± SEM for n = 4–11 for A-E and n = 12–24 data points for F-G. * indicates $p < 0.05$ and *** indicates $p < 0.0001$ versus littermate controls. The annotated p value was calculated by two-way ANOVA for D and E, and by linear regression analysis for F-G. The 95% confidence bands of the best-fit line are shown for F and G.

signaling in adipose tissue are due, at least in part, to an increase in insulin release consequent to increased lipolysis. This highlights the importance of Gs signaling in an adipose tissue-pancreas crosstalk.

3.3. Chemogenetic stimulation of Gs signaling induces the expression of distinctive genes in different adipose depots

We next sought to determine the impact of chemogenetic stimulation of Gs signaling in adipocytes on the expression of key metabolic genes in adipose tissue. Because *salt inducible kinase* (*Sik1*) was previously reported to be rapidly induced following GsD activation [30], we first validated that *Sik1* expression was increased in eWAT, iWAT, and BAT. Validating the efficiency of our approach, *Sik1* mRNA was induced 3- to 8-fold in these adipose depots 6 h following CNO administration (Figure 3A). We next looked at genes involved in lipid metabolism and found important distinctions between the different adipose depots. While the hormone-sensitive lipase (HSL) gene *Lipe* was induced in every depot (Figure 3B), *diacylglycerol o-acyltransferase 1* (*Dgat1*) expression was induced in eWAT but reduced in iWAT (Figure 3C). We also observed an increase in *peroxisome proliferator-activated receptor gamma coactivator a-alpha* (*Ppargc1a*) in every adipose tissue (Figure 3D) and a significant increase in *Ucp1* in iWAT and BAT (Figure 3E). These results suggest that Gs signaling in eWAT induces lipid turnover by stimulating both the lipolytic and lipogenic pathways, whereas Gs stimulation promotes oxidative metabolism in iWAT and BAT. We also found that *TANK binding kinase 1* (*Tbk1*), a gene known to be readily induced by dynamic challenges in adipose tissue [40,41] was increased following Gs stimulation (Figure 3F). Finally, we looked at the impact of adipose Gs signaling on adipokine transcription. Interestingly, *leptin* (*Lep*) expression showed distinctive patterns in eWAT, iWAT, and BAT (Figure 3G). In contrast, adiponectin (*Adipoq*) expression did not change following CNO administration (Figure 3H). We did not observe any significant differences in adipose tissue morphology or adipocyte size between genotypes 24 h after CNO administration (Fig. S3). Together, these data demonstrate the previously unappreciated variation across adipose tissues following Gs signaling stimulation and highlight the usefulness of chemogenetic technology to better understand adipocyte functions.

3.4. Chemogenetic stimulation of Gs signaling stimulates lipolysis *ex vivo*

The *Adipoq*-Cre mouse model has been shown by many groups [34,42,43] to be highly specific to adipose tissue. Although not as ubiquitously expressed as *fatty acid binding protein 4* (*Fabp4/aP2*) [44,45], publicly available bioinformatic data suggests that *Adipoq* is also expressed in the adrenal glands [46,47], which are known to produce hormones influencing metabolism. Moreover, CNO can be back-transformed into clozapine in the liver, which can have systemic effects [48]. We thus decided to modify a widely-used protocol for measuring lipolysis *ex vivo* in adipose tissue explants [36] in order to evaluate the direct impact of CNO on NEFA and glycerol release, as surrogates of lipolysis. As shown in Figure 4A–B, CNO was only effective at increasing NEFA and glycerol release in explants from *Adipoq*-GsD mice. Importantly, no differences were observed at baseline between *Adipoq*-GsD and littermate explants (Supplementary Table 1), indicating that the endogenous expression of the GsD does not affect basal lipolytic rate. As expected, eWAT explants were the

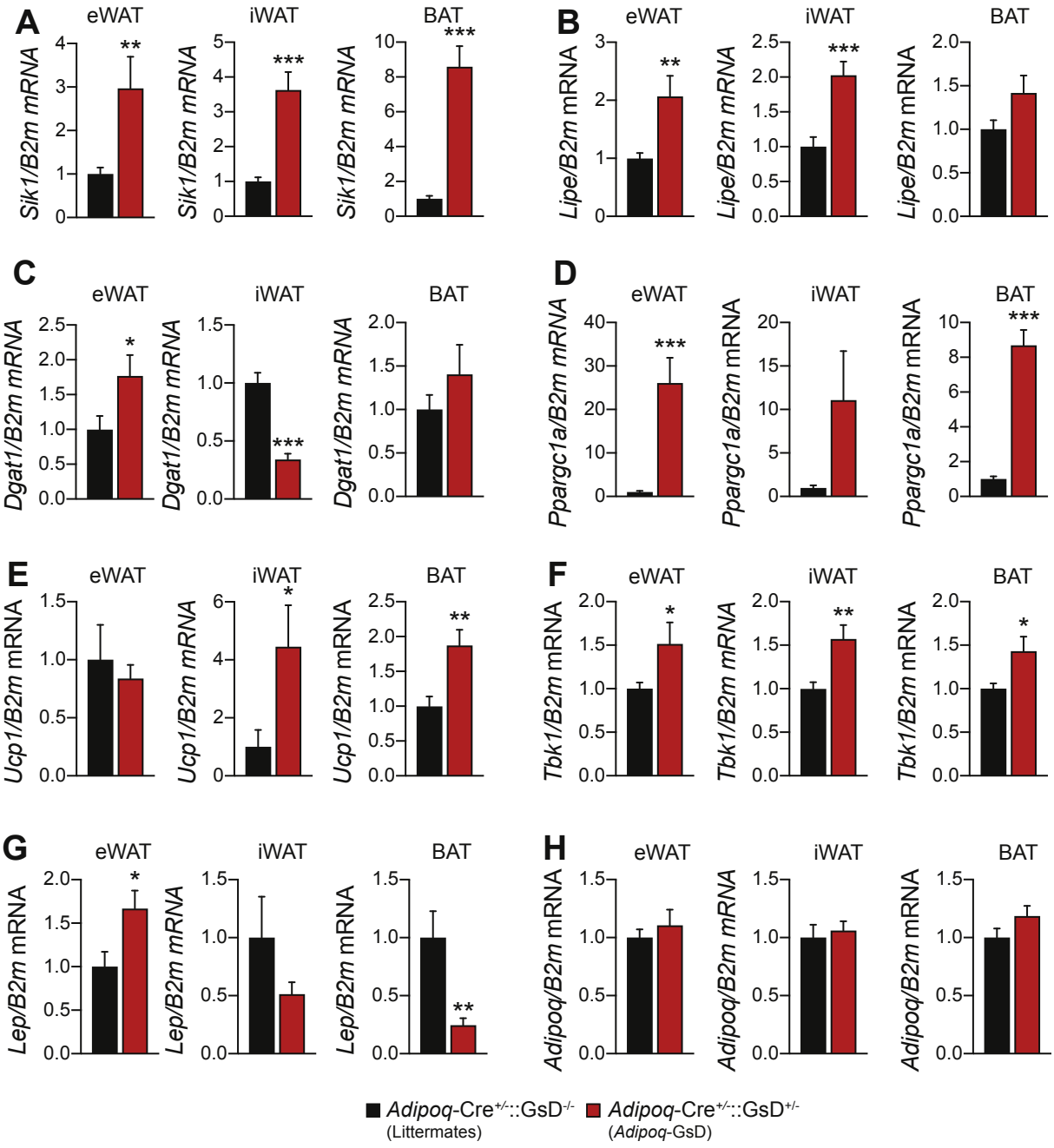

Figure 3: Chemogenetic stimulation of Gs signaling induces the expression of distinctive genes in different adipose depots. Gene expression as assessed by qPCR in eWAT (left), iWAT (middle) and BAT (right) for (A) *Sik1*, (B) *Lipe*, (C) *Dgat1*, (D) *Ppargc1a*, (E) *Ucp1*, (F) *Tbk1*, (G) *Lep*, and (H) *Adipoq*. Tissues were collected 6 h following CNO (1 mg/kg) administration. *B2m* was used as the housekeeping gene. The data are expressed in fold increase as the mean ± SEM for n = 6–8. * indicates $p < 0.05$, ** indicates $p < 0.01$ and *** indicates $p < 0.0001$ versus littermate controls.

most responsive to CNO in terms of fold increase of NEFA and glycerol release, whereas BAT explants were the least responsive. Because ADRB3 and downstream cAMP are well-known to affect leptin levels [10], we also evaluated leptin release in the explants [28]. We found that acute stimulation of Gs signaling in adipose explants does not potently affect leptin release (Figure 4C). Supporting this observation, we did not find any changes in leptin levels following CNO administration (data not shown). Together, these data highlight the efficacy of the *Adipoq*-GsD model to specifically increase lipolysis in an adipose-autonomous manner.

3.5. Chemogenetic stimulation of Gi signaling does not affect glucose homeostasis but stimulates leptin production

Evidence suggests that Gs and Gi signaling have opposing actions in adipose tissue [26,49]. For instance, pharmacological activation of Gs-coupled ADRB3 stimulates lipolysis, whereas pharmacological stimulation of Gi-coupled ADRA2 or stimulation of the lactate receptor GPR81 inhibits lipolysis [49,50]. In order to test whether acute stimulation of Gi signaling in adipocytes has the opposite effect on glucose metabolism as Gs stimulation, we crossed *Adipoq*-Cre mice [34] with Cre-dependent hM4Di-coupled DREADD mice [35] and generated

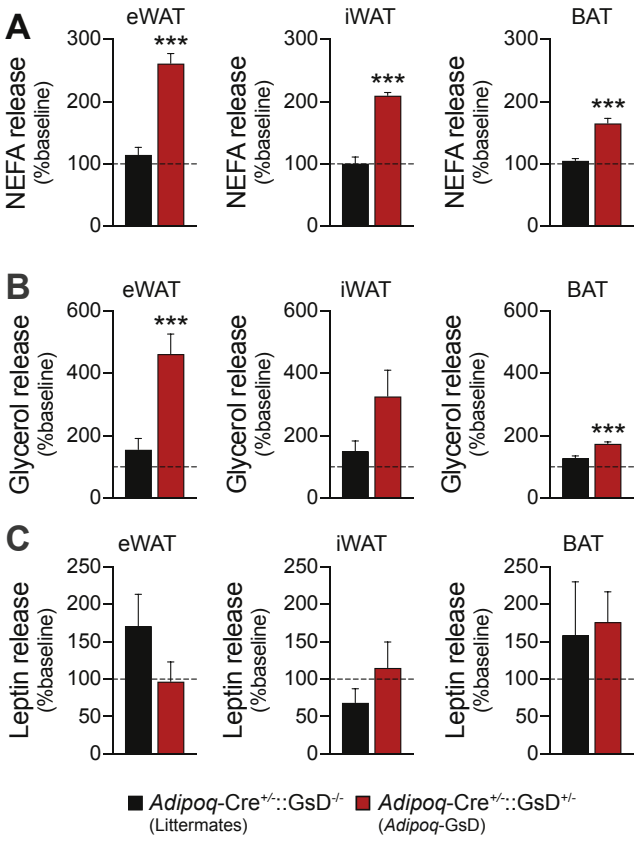

Figure 4: Chemogenetic stimulation of Gs signaling stimulates lipolysis *ex vivo*. (A) NEFA, (B) glycerol, and (C) leptin release from eWAT (left), iWAT (middle) and BAT (right) explants. The data are expressed in % versus baseline as described in the Methods as the mean ± SEM for n = 5–14 replicates from n = 3 animals per group. *** indicates $p < 0.0001$ versus littermate controls. Dashed lines represent baseline.

Adipoq-GiD mice. We first validated the expression of *GiD* in the different adipose depots (Fig. S4A). As shown in Fig. S4B–E, no difference in the expression of endogenous Gi proteins was observed (G Protein Subunit Alpha I1, *Gnai1*, G Protein Subunit Alpha I2, *Gnai2*, G Protein Subunit Alpha I3, *Gnai3*, and G Protein Subunit Alpha Z, *Gnaz*). Likewise, we did not observe any difference in body composition, food intake and energy expenditure (Fig. S2F–J). In contrast to what we observed with Gs stimulation, we did not observe any effect of CNO on glucose levels in *Adipoq*-GiD (Figure 5A–B). Moreover, pre-stimulation of Gi signaling with CNO did not prevent the hypoglycemic effects of a low dose of CL316,243 (Fig. S5). Based on evidence suggesting that pharmacological stimulation of the Gi-coupled ADRA2 increases leptin levels [28], we next tested whether chemogenetic stimulation of adipose Gi signaling affects leptin production. As shown in Figure 5C–D, we observed a modest but significant increase in plasma leptin levels 2 h following CNO administration in *Adipoq*-GiD mice compared to littermate controls. We did not find any difference in the expression of *Lipe* or *Ppargc1a* in eWAT, iWAT, and BAT (Figure 6A–B), suggesting that the GiD stimulation did not affect lipolysis or oxidation. Furthermore, CNO did not affect NEFA release (Figure 6C) in adipose explants, suggesting that acute stimulation of adipocyte Gi signaling does not impair lipolysis. Together, these results suggest that acute stimulation of Gi signaling in adipose tissue does not affect glucose metabolism or lipolysis, but contributes to the regulation of leptin production. Collectively, our data highlight the complexity of GPCR signaling in adipose tissue.

4. DISCUSSION

Because of their pleiotropic effects on energy and glucose homeostasis, targeting adipose GPCRs represents a potential approach to treat obesity and diabetes [4–6]. In particular, the Gs-coupled ADRB3 has emerged as a conceivable target due to its effects on lipolysis, thermogenesis, and browning [4]. Recent work also suggests an important network of non-adrenergic GPCR in the regulation of adipose tissue biology [6,19,24]. Gi-coupled ADRA2 are considered to oppose the stimulation of lipolysis by ADRB3 by reducing cAMP levels [25,26] and recent work highlights the importance of the ADRB3/ADRA2 balance in controlling leptin production [27,28]. Here, we report the generation of novel chemogenetic tools allowing acute stimulation of Gs and Gi signaling in adipocytes and highlight different outcomes that stimulating these pathways have in distinct adipose depots.

Our data indicate a potentially important role for adipose Gs signaling in regulating glucose homeostasis. Chemogenetic stimulation of adipose Gs was sufficient at lowering blood glucose in less than 20 min, an effect that was sustained for hours. The decrease in glucose levels may be secondary to uptake in the adipose depots. However, we found that chemogenetic stimulation of adipose Gs signaling drastically improved glucose clearance and increased insulin secretion, suggesting that insulin-mediated glucose uptake in other tissues including muscles might also play an important role in the hypoglycemic phenotype. Importantly, the hypoglycemic effects of CNO in *Adipoq*-GsD animals were similar to an insulin bolus in littermate controls. These results are in line with previous observations that acute pharmacological stimulation of ADRB3 results in increased insulin levels and decreased glycemia [5,51]. Consistent with the use of an ADRB3 agonist [5,39], our data suggest that the incretin effects of Gs signaling are consequent to increased lipolysis. This idea is reinforced by a strong negative correlation between blood glucose and plasma NEFA in *Adipoq*-GsD but not littermate controls. Exactly how adipose tissue Gs signaling regulates insulin secretion is still unclear. Supporting our findings, previous work has suggested that the effects of CL316,243 on insulin secretion are secondary to increased plasma NEFA [5,39]. Importantly, inhibiting lipolysis with nicotinic acid was shown to blunt the CL316,243-mediated increase in insulin levels [5]. Moreover, mice lacking ATGL, a rate-limiting enzyme of lipolysis, fail to exhibit hyperinsulinemia following pharmacological stimulation of ADRB3 [5,39]. Interestingly, mice lacking the free fatty acid receptor GPR40, which is expressed by pancreatic beta cells, have a blunted hyperinsulinemic response to CL 316,243 [52]. However, deletion of GPR40 only reduces the effects of CL 316,243 by 50%, suggesting that additional mechanisms mediate the effect of ADRB3 stimulation on insulin levels [52]. Therefore, we believe that additional factors (e.g. secretion of adipokines) might explain the effects of adipose Gs stimulation on insulin release. Another possibility is that the stimulation of adipocyte Gs signaling may stimulate a neuronal afferent communication to the brain and subsequent efferent output to pancreas. This idea is supported by the existence of an important afferent network between adipose tissue and the central nervous system [11,53,54], as well as an efferent pathway regulating insulin secretion [55]. Together, our results suggest that pharmacological targeting of Gs signaling in adipose tissue represents a potential avenue for the management of hyperglycemia in type 2 diabetes patients. Additional studies are needed to better understand how exactly the acute stimulation of Gs signaling results in an adipose tissue-pancreas crosstalk and to define whether the benefits of stimulating adipocyte Gs signaling can be harnessed in disease models.

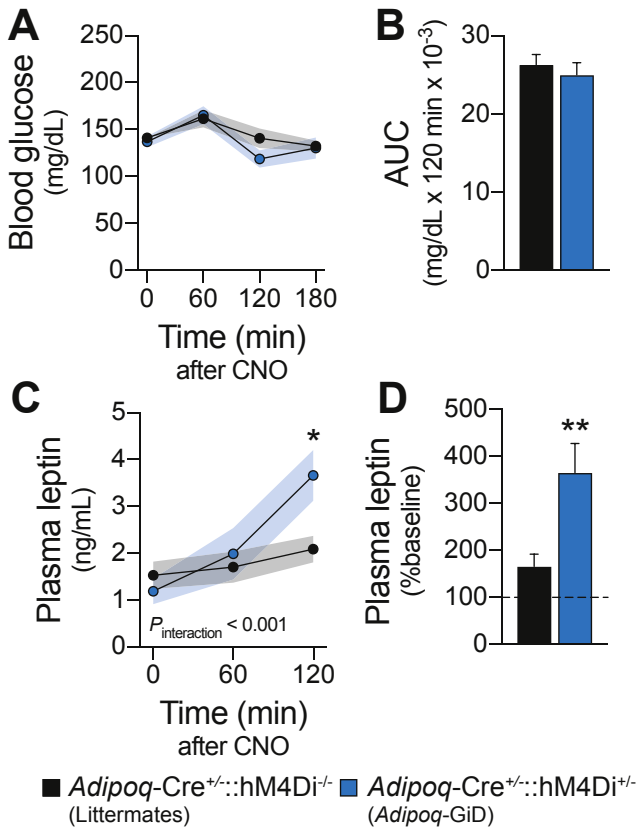

Figure 5: Chemogenetic stimulation of Gi signaling does not affect glucose homeostasis but stimulates leptin production. (A) Blood glucose measured every hour for 3 h following CNO (1 mg/kg) in *Adipoq*-GiD and littermate controls. (B) AUC for A. C) Plasma leptin levels following CNO (1 mg/kg). (D) Plasma leptin levels 2 h following CNO expressed as % baseline from (C). The data are expressed as the mean ± SEM for n = 5–10. * indicated $p < 0.05$ and ** indicates $p < 0.01$ versus littermate controls. The annotated p value was calculated by two-way ANOVA. Dashed lines represent baseline.

In addition to the potent effects on glucose homeostasis, we found important distinctions between the different adipose depots in terms of gene expression profile. Our data suggest that despite somewhat similar activation of HSL and CREB pathways, as evidenced by increase in the expression of *Lipe*, *Ppargc1a*, and *Sik1* in eWAT, iWAT, and BAT, Gs stimulation did not affect other genes the same way. For instance, *Dgat1,* which encodes the protein catalyzing the conversion of diacylglycerol and fatty acyl (FA) CoA to triacylglycerol (TG), was upregulated in eWAT but downregulated in iWAT. Interestingly, the effects of fasting and re-feeding on *Dgat1* expression in different adipose depots was previously shown to follow a similar pattern, with *Dgat1* being downregulated upon fasting [56]. Moreover, DGAT1 is suggested to be key for re-esterifying FA back to TG during lipolysis to protect the endoplasmic reticulum from lipotoxic stress [56]. It is tempting to speculate that the rapid lipid turnover caused by Gs stimulation in eWAT results in increased DGAT1 activity for these same reasons. The use of Cre lines that allow the targeting of eWAT but not iWAT, such as the *Wilms Tumor one locus* (*Wt1*-Cre) [57,58], will be key to better understand the role of Gs signaling in regulating this particular adipose depot. Another important distinction was the expression of *Ucp1*, which was upregulated in iWAT and BAT but not in eWAT. Because eWAT is considered resistant to browning following acute adrenergic stimulation [58], these results suggest that Gs signaling promotes the browning of iWAT and stimulates the thermogenic machinery of both brown and brite adipocytes, similar to an ADRB3 stimulation [14,59]. On the other hand, in visceral adipose tissues such as eWAT, Gs signaling potently stimulates lipid mobilization and re-esterification by forcing profound lipid turnover. The fact that we did not observe important histological difference in iWAT and BAT between *Adipoq*-GsD and littermates is quite surprising, but it supports the absence of effects on energy expenditure. One possible explanation is that although a single injection of CNO promotes the oxidative/thermogenic capacity (gene expression) of these organs, additional inputs are needed to stimulate iWAT and BAT oxidative/thermogenic activity. This is supported by previous literature showing important distinctions between oxidative/thermogenic capacity and activity [14,60,61]. It is also plausible that chronic CNO administration potentiates the browning of iWAT and energy expenditure, which is beyond the scope of our acute GPCR stimulation studies. However, chronic treatment with high doses of CNO are associated with many adverse effects [62], mostly due to its back-transformation into clozapine [48], that could limit the attractiveness to such an approach. Nonetheless, these

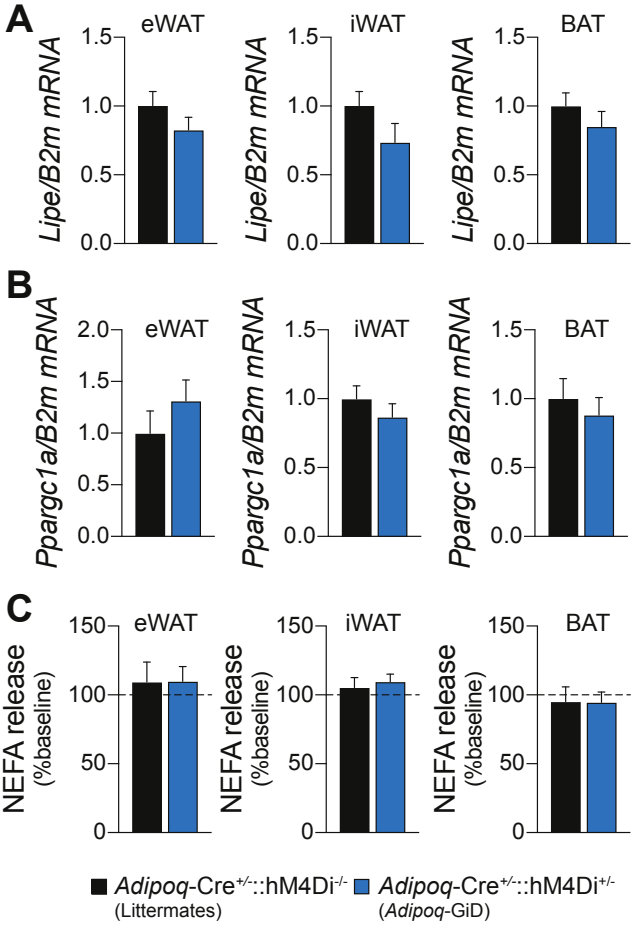

Figure 6: Chemogenetic stimulation of Gi signaling does not affect lipid mobilization. Gene expression as assessed by qPCR in eWAT (left), iWAT (middle) and BAT (right) for (A) *Lipe* and (B) *Ppargc1a.* Tissues were collected 6 h following CNO (1 mg/kg) administration. *B2m* was used as the housekeeping gene. The data are expressed in fold increase as the mean ± SEM for n = 8–12. (C) NEFA release from eWAT (left), iWAT (middle) and BAT (right) explants. The data are expressed in % versus baseline as described in the Methods as the mean ± SEM for n = 3–8 replicates from n = 4 animals per group. Dashed lines represent baseline.

chemogenetic approaches will be invaluable tools for chronically or acutely controlling these pathways in a spatiotemporal manner.

One surprising observation was the absence of effects on lipolysis in the GiD model. Previous work indicates that Gi-coupled ADRA2 opposes the stimulation of lipolysis by ADRB3 by reducing cAMP levels [25,26]. Moreover, deletion of Gi-coupled GPR43 and GPR81 was shown to have significant effects on lipolysis [50,63]. Our results suggest that acute stimulation of Gi signaling does not impair baseline lipolysis. One possible explanation for this discrepancy is that at the time of Gi stimulation, there was no Gs signaling and therefore no cAMP available for degradation nor adenylyl cyclase that needed to be blocked. Another notable distinction is that our chemogenetic approach leads to an acute stimulation of a particular pathway, whereas global knock-out models involve the permanent deletion of a gene that, if deleted early in life, can lead to developmental compensation. Together, these results highlight how combining chemogenetic tools with pharmacology and transgenic mouse models will lead to a better understanding of the complex biology of GPCR signaling.

Previous studies have shown that pharmacological stimulation of ADRB3 [64–70] suppresses leptin levels and *Lep* expression. Here, we found that following Gs stimulation, *Lep* mRNA expression was increased in eWAT and decreased in BAT, with no impact on leptin release *ex vivo*. These results suggest that the effects of ADRB3 on reducing leptin transcription may be Gs independent. This is supported by evidence that ADRB3 show a dynamic capacity to stimulate divergent G proteins. For example, ADRB3 stimulates the mitogen-activated protein kinase (AMPK)/extracellular signal-regulated kinases (ERK) pathway in adipocytes through a Gi-dependent mechanism [71,72]. Moreover, adrenergic stimulation (presumably through ADRB3) was shown to not only trigger the cAMP-PKA pathway, but also to influence phosphoinositide 3-kinase (PI3K) and protein kinase C (PKC) in brown adipocytes [73]. It is noteworthy that overexpression of ADRA2 in *Adrb3* knock-out mouse adipose tissue increases leptin levels [27]. In addition, pharmacological stimulation of ADRA2 increases leptin levels [28]. Here, we show that *Adipoq*-GiD mice but not littermate controls exhibit modest but significant increase in plasma leptin two hours following CNO administration. Thus, the Gi/Gs balance in adipocytes appears to be key for the regulation of leptin and we believe that these chemogenetic tools will allow a better understanding of the roles of G proteins in adipose tissue *in vivo*.

5. CONCLUSION

In conclusion, our data demonstrate the importance of adipose Gs signaling in regulating systemic glucose homeostasis. We found notable differences in the gene expression profile of distinct adipose depots in response to Gs stimulation. In contrast, we found that Gi signaling had no effect on glucose metabolism, but increased circulating leptin levels. Together, our data highlight the complexity of GPCR signaling in adipose tissue and demonstrate the usefulness of chemogenetic technology to better understand adipocyte functions.

AUTHORS CONTRIBUTION

Conceptualization, AC and JKE; Methodology, AC, RPR, CMC, NJM, and CEL; Formal Analysis, AC and RPR; Investigation, AC, RPR, CMC, and NJM; Writing — Original Draft, AC and JKE; Writing — Review & Editing, AC, SL, PES, and JKE; Funding Acquisition, PES and JKE; Supervision, PES and JKE; Resources, PES and JKE. All authors contributed to editing the manuscript and approved the manuscript for publication.

ACKNOWLEDGEMENTS

We thank the NIH for its support (RO1 DK118725, K99 DK120894, K01 DK111644, R01 DK092590 and R01 AR059847). AC is a Canadian Institutes of Health Research (CIHR) Banting fellow.

CONFLICT OF INTEREST

The authors declare no conflicts of interest.

APPENDIX A. SUPPLEMENTARY DATA

Supplementary data to this article can be found online at https://doi.org/10.1016/j.molmet.2019.06.019.

REFERENCES

[1] Hauser, A.S., Attwood, M.M., Rask-Andersen, M., Schioth, H.B., Gloriam, D.E., 2017. Trends in GPCR drug discovery: new agents, targets and indications. Nature Reviews Drug Discovery 16(12):829–842.

[2] Lefkowitz, R.J., 2007. Seven transmembrane receptors: something old, something new. Acta Physiologica 190(1):9–19.

[3] Gilman, A.G., 1987. G proteins: transducers of receptor-generated signals. Annual Review of Biochemistry 56:615–649.

[4] Cypess, A.M., Weiner, L.S., Roberts-Toler, C., Elia, E.F., Kessler, S.H., Kahn, P.A., et al., 2015. Activation of human brown adipose tissue by a β3-adrenergic receptor agonist. Cell Metabolism 21(1):33–38.

[5] MacPherson, R.E., Castellani, L., Beaudoin, M.S., Wright, D.C., 2014. Evidence for fatty acids mediating CL 316,243-induced reductions in blood glucose in mice. American Journal of Physiology. Endocrinology and Metabolism 307(7): E563–E570.

[6] Li, Y., Schnabl, K., Gabler, S.M., Willershauser, M., Reber, J., Karlas, A., et al., 2018. Secretin-activated brown fat mediates prandial thermogenesis to induce satiation. Cell 175(6):1561–1574 e12.

[7] Chechi, K., Carpentier, A.C., Richard, D., 2013. Understanding the brown adipocyte as a contributor to energy homeostasis. Trends in Endocrinology and Metabolism 24(8):408–420.

[8] Rosen, E.D., Spiegelman, B.M., 2014. What we talk about when we talk about fat. Cell 156(1–2):20–44.

[9] Harms, M., Seale, P., 2013. Brown and beige fat: development, function and therapeutic potential. Nature Medicine 19(10):1252–1263.

[10] Caron, A., Lee, S., Elmquist, J.K., Gautron, L., 2018. Leptin and brain–adipose crosstalks. Nature Reviews Neuroscience 19(3):153–165.

[11] Bartness, T.J., Liu, Y., Shrestha, Y.B., Ryu, V., 2014. Neural innervation of white adipose tissue and the control of lipolysis. Frontiers in Neuroendocrinology 35(4):473–493.

[12] Labbe, S.M., Caron, A., Lanfray, D., Monge-Rofarello, B., Bartness, T.J., Richard, D., 2015. Hypothalamic control of brown adipose tissue thermogenesis. Frontiers in Systems Neuroscience 9:150.

[13] Nakamura, K., Morrison, S.F., 2011. Central efferent pathways for cold-defensive and febrile shivering. Journal of Physiology 589(Pt 14):3641–3658.

[14] Labbé, S.M., Caron, A., Chechi, K., Laplante, M., Lecomte, R., Richard, D., 2016. Metabolic activity of brown,"beige", and white adipose tissues in response to chronic adrenergic stimulation in male mice. American Journal of Physiology-Endocrinology and Metabolism 311(1):E260–E268.

[15] Brito, N.A., Brito, M.N., Bartness, T.J., 2008. Differential sympathetic drive to adipose tissues after food deprivation, cold exposure or glucoprivation. American Journal of Physiology - Regulatory, Integrative and Comparative Physiology 294(5):R1445–R1452.

[16] Rayner, D.V., 2001. The sympathetic nervous system in white adipose tissue regulation. Proceedings of the Nutrition Society 60(3):357–364.

[17] Bartness, T.J., Vaughan, C.H., Song, C.K., 2010. Sympathetic and sensory innervation of brown adipose tissue. International Journal of Obesity 34(Suppl. 1):S36–S42.

[18] Ueta, C.B., Fernandes, G.W., Capelo, L.P., Fonseca, T.L., Maculan, F.D., Gouveia, C.H., et al., 2012. β1 Adrenergic receptor is key to cold- and diet-induced thermogenesis in mice. Journal of Endocrinology 214(3):359–365.

[19] Braun, K., Oeckl, J., Westermeier, J., Li, Y., Klingenspor, M., 2018. Non-adrenergic control of lipolysis and thermogenesis in adipose tissues. Journal of Experimental Biology 221(Pt Suppl. 1).

[20] Warner, A., Kjellstedt, A., Carreras, A., Bottcher, G., Peng, X.R., Seale, P., et al., 2016. Activation of β3-adrenoceptors increases in vivo free fatty acid uptake and utilization in brown but not white fat depots in high-fat-fed rats. American Journal of Physiology. Endocrinology and Metabolism 311(6): E901–E910.

[21] Umekawa, T., Yoshida, T., Sakane, N., Saito, M., Kumamoto, K., Kondo, M., 1997. Anti-obesity and anti-diabetic effects of CL316,243, a highly specific β3-adrenoceptor agonist, in Otsuka Long-Evans Tokushima Fatty rats: induction of uncoupling protein and activation of glucose transporter 4 in white fat. European Journal of Endocrinology 136(4):429–437.

[22] Li, Y.Q., Shrestha, Y.B., Chen, M., Chanturiya, T., Gavrilova, O., Weinstein, L.S., 2016. Gsα deficiency in adipose tissue improves glucose metabolism and insulin sensitivity without an effect on body weight. Proceedings of the National Academy of Sciences of the United States of America 113(2):446–451.

[23] Chen, M., Chen, H., Nguyen, A., Gupta, D., Wang, J., Lai, E.W., et al., 2010. G(s)α deficiency in adipose tissue leads to a lean phenotype with divergent effects on cold tolerance and diet-induced thermogenesis. Cell Metabolism 11(4):320–330.

[24] Schnabl, K., Westermeier, J., Li, Y., Klingenspor, M., 2018. Opposing actions of adrenocorticotropic hormone and glucocorticoids on UCP1-mediated respiration in brown adipocytes. Frontiers in Physiology 9:1931.

[25] Lafontan, M., Berlan, M., 1993. Fat cell adrenergic receptors and the control of white and brown fat cell function. The Journal of Lipid Research 34(7): 1057–1091.

[26] Garg, A., Sankella, S., Xing, C., Agarwal, A.K., 2016. Whole-exome sequencing identifies ADRA2A mutation in atypical familial partial lipodystrophy. JCI Insight 1(9).

[27] Valet, P., Grujic, D., Wade, J., Ito, M., Zingaretti, M.C., Soloveva, V., et al., 2000. Expression of human α2-adrenergic receptors in adipose tissue of β3-adrenergic receptor-deficient mice promotes diet-induced obesity. Journal of Biological Chemistry 275(44):34797–34802.

[28] Caron, A., Dungan Lemko, H.M., Castorena, C.M., Fujikawa, T., Lee, S., Lord, C.C., et al., 2018. POMC neurons expressing leptin receptors coordinate metabolic responses to fasting via suppression of leptin levels. Elife 7.

[29] Roth, B.L., 2016. DREADDs for neuroscientists. Neuron 89(4):683–694.

[30] Akhmedov, D., Mendoza-Rodriguez, M.G., Rajendran, K., Rossi, M., Wess, J., Berdeaux, R., 2017. Gs-DREADD knock-in mice for tissue-specific, temporal stimulation of cAMP signaling. Molecular and Cellular Biology.

[31] Rossi, M., Zhu, L., McMillin, S.M., Pydi, S.P., Jain, S., Wang, L., et al., 2018. Hepatic Gi signaling regulates whole-body glucose homeostasis. Journal of Clinical Investigation 128(2):746–759.

[32] Kaiser, E., Tian, Q., Wagner, M., Barth, M., Xian, W., Schroeder, L., et al., 2018. DREADD technology reveals major impact of Gq signaling on cardiac electrophysiology. Cardiovasc Res.

[33] Guettier, J.M., Gautam, D., Scarselli, M., Ruiz de Azua, I., Li, J.H., Rosemond, E., et al., 2009. A chemical-genetic approach to study G protein regulation of beta cell function in vivo. Proceedings of the National Academy of Sciences of the United States of America 106(45):19197–19202.

[34] Eguchi, J., Wang, X., Yu, S., Kershaw, E.E., Chiu, P.C., Dushay, J., et al., 2011. Transcriptional control of adipose lipid handling by IRF4. Cell Metabolism 13(3):249–259.

[35] Zhu, H., Aryal, D.K., Olsen, R.H., Urban, D.J., Swearingen, A., Forbes, S., et al., 2016. Cre-dependent DREADD (designer receptors exclusively activated by designer Drugs) mice. Genesis 54(8):439–446.

[36] Schweiger, M., Eichmann, T.O., Taschler, U., Zimmermann, R., Zechner, R., Lass, A., 2014. Measurement of lipolysis. Methods in Enzymology 538: 171–193.

[37] Miller, R.A., Birnbaum, M.J., 2016. Glucagon: acute actions on hepatic metabolism. Diabetologia 59(7):1376–1381.

[38] Collins, S., Daniel, K.W., Petro, A.E., Surwit, R.S., 1997. Strain-specific response to β_3-adrenergic receptor agonist treatment of diet-induced obesity in mice. Endocrinology 138(1):405–413.

[39] Heine, M., Fischer, A.W., Schlein, C., Jung, C., Straub, L.G., Gottschling, K., et al., 2018. Lipolysis triggers a systemic insulin response essential for efficient energy replenishment of activated Brown adipose tissue in mice. Cell Metabolism 28(4):644–655 e4.

[40] Chiang, S.H., Bazuine, M., Lumeng, C.N., Geletka, L.M., Mowers, J., White, N.M., et al., 2009. The protein kinase IKKepsilon regulates energy balance in obese mice. Cell 138(5):961–975.

[41] Zhao, P., Wong, K.I., Sun, X., Reilly, S.M., Uhm, M., Liao, Z., et al., 2018. TBK1 at the crossroads of inflammation and energy homeostasis in adipose tissue. Cell 172(4):731–743 e12.

[42] Mullican, S.E., Tomaru, T., Gaddis, C.A., Peed, L.C., Sundaram, A., Lazar, M.A., 2013. A novel adipose-specific gene deletion model demonstrates potential pitfalls of existing methods. Molecular Endocrinology 27(1):127–134.

[43] Wang, Q.A., Scherer, P.E., Gupta, R.K., 2014. Improved methodologies for the study of adipose biology: insights gained and opportunities ahead. The Journal of Lipid Research 55(4):605–624.

[44] Lee, K.Y., Russell, S.J., Ussar, S., Boucher, J., Vernochet, C., Mori, M.A., et al., 2013. Lessons on conditional gene targeting in mouse adipose tissue. Diabetes 62(3):864–874.

[45] Harno, E., Cottrell, E.C., White, A., 2013. Metabolic pitfalls of CNS Cre-based technology. Cell Metabolism 18(1):21–28.

[46] Wu, C., Orozco, C., Boyer, J., Leglise, M., Goodale, J., Batalov, S., et al., 2009. BioGPS: an extensible and customizable portal for querying and organizing gene annotation resources. Genome Biology 10(11):R130.

[47] Consortium, E.P., 2012. An integrated encyclopedia of DNA elements in the human genome. Nature 489(7414):57–74.

[48] Gomez, J.L., Bonaventura, J., Lesniak, W., Mathews, W.B., Sysa-Shah, P., Rodriguez, L.A., et al., 2017. Chemogenetics revealed: DREADD occupancy and activation via converted clozapine. Science 357(6350):503–507.

[49] Lafontan, M., Berlan, M., 1995. Fat cell α_2-adrenoceptors: the regulation of fat cell function and lipolysis. Endocrine Reviews 16(6):716–738.

[50] Liu, C., Wu, J., Zhu, J., Kuei, C., Yu, J., Shelton, J., et al., 2009. Lactate inhibits lipolysis in fat cells through activation of an orphan G-protein-coupled receptor, GPR81. Journal of Biological Chemistry 284(5):2811–2822.

[51] Labbe, S.M., Mouchiroud, M., Caron, A., Secco, B., Freinkman, E., Lamoureux, G., et al., 2016. mTORC1 is required for brown adipose tissue recruitment and metabolic adaptation to cold. Scientific Reports 6:37223.

[52] Pang, Z., Wu, N., Zhang, X., Avallone, R., Croci, T., Dressler, H., et al., 2010. GPR40 is partially required for insulin secretion following activation of β3-adrenergic receptors. Molecular and Cellular Endocrinology 325(1–2):18–25.

[53] Ryu, V., Bartness, T.J., 2014. Short and long sympathetic-sensory feedback loops in white fat. American Journal of Physiology - Regulatory, Integrative and Comparative Physiology 306(12):R886–R900.

[54] Bartness, T.J., Shrestha, Y.B., Vaughan, C.H., Schwartz, G.J., Song, C.K., 2010. Sensory and sympathetic nervous system control of white adipose tissue lipolysis. Molecular and Cellular Endocrinology 318(1–2):34–43.

[55] Thorens, B., 2011. Brain glucose sensing and neural regulation of insulin and glucagon secretion. Diabetes, Obesity and Metabolism 13(Suppl. 1):82–88.

[56] Chitraju, C., Mejhert, N., Haas, J.T., Diaz-Ramirez, L.G., Grueter, C.A., Imbriglio, J.E., et al., 2017. Triglyceride synthesis by DGAT1 protects

adipocytes from lipid-induced ER stress during lipolysis. Cell Metabolism 26(2):407—418 e3.

[57] Chau, Y.Y., Bandiera, R., Serrels, A., Martinez-Estrada, O.M., Qing, W., Lee, M., et al., 2014. Visceral and subcutaneous fat have different origins and evidence supports a mesothelial source. Nature Cell Biology 16(4):367—375.

[58] Hepler, C., Shao, M., Xia, J.Y., Ghaben, A.L., Pearson, M.J., Vishvanath, L., et al., 2017. Directing visceral white adipocyte precursors to a thermogenic adipocyte fate improves insulin sensitivity in obese mice. Elife 6.

[59] Labbe, S.M., Caron, A., Bakan, I., Laplante, M., Carpentier, A.C., Lecomte, R., et al., 2015. In vivo measurement of energy substrate contribution to cold-induced brown adipose tissue thermogenesis. The FASEB Journal 29(5): 2046—2058.

[60] Nedergaard, J., Cannon, B., 2013. UCP1 mRNA does not produce heat. Biochimica et Biophysica Acta 1831(5):943—949.

[61] Labbé, S.M., Caron, A., Festuccia, W.T., Lecomte, R., Richard, D., 2018. Interscapular brown adipose tissue denervation does not promote the oxidative activity of inguinal white adipose tissue in male mice. American Journal of Physiology-Endocrinology and Metabolism 315(5):E815—E824.

[62] Martinez, V.K., Saldana-Morales, F., Sun, J.J., Zhu, P.J., Costa-Mattioli, M., Ray, R.S., 2019. Off-target effects of clozapine-N-oxide on the chemosensory reflex are masked by high stress levels. Frontiers in Physiology 10:521.

[63] Ge, H., Li, X., Weiszmann, J., Wang, P., Baribault, H., Chen, J.L., et al., 2008. Activation of G protein-coupled receptor 43 in adipocytes leads to inhibition of lipolysis and suppression of plasma free fatty acids. Endocrinology 149(9): 4519—4526.

[64] Moinat, M., Deng, C., Muzzin, P., Assimacopoulos-Jeannet, F., Seydoux, J., Dulloo, A.G., et al., 1995. Modulation of obese gene expression in rat brown and white adipose tissues. FEBS Letters 373(2):131—134.

[65] Trayhurn, P., Duncan, J.S., Rayner, D.V., Hardie, L.J., 1996. Rapid inhibition of ob gene expression and circulating leptin levels in lean mice by the β3-adrenoceptor agonists BRL 35135A and ZD2079. Biochemical and Biophysical Research Communications 228(2):605—610.

[66] Gettys, T.W., Harkness, P.J., Watson, P.M., 1996. The beta 3-adrenergic receptor inhibits insulin-stimulated leptin secretion from isolated rat adipocytes. Endocrinology 137(9):4054—4057.

[67] Deng, C., Moinat, M., Curtis, L., Nadakal, A., Preitner, F., Boss, O., et al., 1997. Effects of beta-adrenoceptor subtype stimulation on obese gene messenger ribonucleic acid and on leptin secretion in mouse brown adipocytes differentiated in culture. Endocrinology 138(2):548—552.

[68] Trayhurn, P., Duncan, J.S., Hoggard, N., Rayner, D.V., 1998. Regulation of leptin production: a dominant role for the sympathetic nervous system? Proceedings of the Nutrition Society 57(3):413—419.

[69] Mantzoros, C.S., Qu, D., Frederich, R.C., Susulic, V.S., Lowell, B.B., Maratos-Flier, E., et al., 1996. Activation of β3 adrenergic receptors suppresses leptin expression and mediates a leptin-independent inhibition of food intake in mice. Diabetes 45(7):909—914.

[70] Giacobino, J.P., 1996. Role of the beta3-adrenoceptor in the control of leptin expression. Hormone and Metabolic Research 28(12):633—637.

[71] Cao, W., Luttrell, L.M., Medvedev, A.V., Pierce, K.L., Daniel, K.W., Dixon, T.M., et al., 2000. Direct binding of activated c-Src to the β3-adrenergic receptor is required for MAP kinase activation. Journal of Biological Chemistry 275(49): 38131—38134.

[72] Soeder, K.J., Snedden, S.K., Cao, W., Della Rocca, G.J., Daniel, K.W., Luttrell, L.M., et al., 1999. The β3-adrenergic receptor activates mitogen-activated protein kinase in adipocytes through a Gi-dependent mechanism. Journal of Biological Chemistry 274(17):12017—12022.

[73] Chernogubova, E., Cannon, B., Bengtsson, T., 2004. Norepinephrine increases glucose transport in brown adipocytes via β_3-adrenoceptors through a cAMP, PKA, and PI3-kinase-dependent pathway stimulating conventional and novel PKCs. Endocrinology 145(1):269—280.

